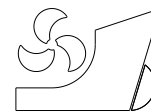*Inmaculada Ortigosa*
Julio García-Espinosa
Marcel·la Castells

A REAL TIME DECISION SUPPORT SYSTEM FOR THE ADJUSTMENT OF SAILBOAT RIGGING

Summary

The operational complexity and performance requirements of modern racing yachts demand the use of advanced applications, such as a decision support system (DSS) able to assist crew members during navigation. In this article, the authors describe a near-time computational solver as the main piece of a DSS which analyses and monitors the behaviour of sails and rigging. The solver is made up of two different interconnected tools: an iterative Fluid-Structure Interaction algorithm and an advanced Wireless Sensor Network to monitor rigging. The real-time DSS quantifies crew manoeuvres in physical terms, which are reproduced by a simulation program. It can be used in the design phase of sailing yachts and as an aid for real-time boat performance optimisation and accident prevention. This novel DSS is a useful tool for navigation, especially in races.

Key words: racing yacht; trim parameters; decision support system; rigging monitoring;

1. Introduction

The enormous improvements made in yacht design in the last decades have resulted in significantly enhanced performance of these vessels. However, growing competitiveness among designers has increased the demand for detailed experimental and computational research to better understand the behaviour of racing yachts and optimise their design. Moreover, the operational complexity and performance requirements of modern racing yachts require the use of advanced applications.

Some applications are used for optimal selection of a mast and standing rigging [1] whereas others focus on the development of expert decision support systems for ship design [2]. Other contributions have addressed computer-aided design of ship systems automation [3, 4, 5 and 6]. Two more examples of applications are a decision support system (DSS) for vessel fleet scheduling [7] and a knowledge-based DSS for shipboard damage control [8].

The above works have helped build the background to ship design, building and management requirements so that research on DSS applied to ship security and control is increased. However, none of these studies are focused on any specific type of ships, e.g. racing yachts.

Sailing is the art of controlling a boat with large foils called sails. A sailor manages the force of the wind on the sails by adjusting the rigging in order to control the direction and speed of the boat. Sails are designed to be able to take the optimal shape for all sailing conditions. To obtain the best sail shape, the crew adjust the traveller position and sail twist and camber. The fluid-structure interaction of sails and rigging is related to these manoeuvres.

The performance of the sail/rigging configuration can be analysed by two aerodynamic parameters, i.e. lift coefficient and drag coefficient. [9] investigated the relation between changes in sail loads and in trim. The results showed that sail turn (change in traveller position) has an effect on lift and drag whereas camber has no influence on the former and only a slight influence on the latter. In order to study the behaviour of sails and rigging during navigation, it is necessary to consider all manoeuvrability variables. No software for operational computation of structure response to wind conditions considering variations in trim parameters introduced by the crew is currently available. One of the motivations of this work was to develop a novel operational navigation tool using variations in trim parameters to support crew decision making.

Structural failures of racing yachts are not infrequent. Just as an example, the Groupama team broke the mast during the last Volvo Ocean race. A real-time monitoring and structure analysis tool could help prevent damage to the structure and injuries to the crew. The automation of emergency management operations is today driven by complex technology architectures called *damage control system* (DSC) [10]. A DCS is an information-retrieval and equipment-control system that gives ship personnel the ability to detect, analyse and handle various types of damage situations based on the collection and processing of vast quantities of shipboard information. However, no DCS addressed specifically designed for sailing yachts has yet been developed.

The main goal of this article is to present an operational tool that can be the main piece of a decision support system (DSS) to assist the sailing yacht crew during navigation, as well as to prevent accidents, just as a DCS does.

Our work focuses on the development of a program for monitoring/simulation of the behaviour of upwind sails and rigging which helps the crew optimise real-time yacht performance. Rigging is monitored to obtain the boat structure trim introduced by the crew, and the aerodynamic coefficients and structure response to wind conditions and trim, which is valuable information for the crew, are computed.

The monitoring/simulation program requires the development of a solver composed of two interrelated tools:
- A Wireless Sensor Network (WSN) to monitor rigging and sails and capture trim.
- A Fluid-Structure Interaction (FSI) algorithm to compute the performance of sail/rigging configurations. It integrates two solvers: (1) a fluid dynamics solver based on the Boundary Element Method (BEM) [11] to calculate the aerodynamic forces for a given sail shape in upwind conditions; (2) a Finite Element Analysis (FEA) solver [12 and 13] of the structural behaviour of rigging and sails which considers aerodynamic forces and shroud and stay tension, as well as sheet tension.

The WSN quantifies crew manoeuvres in physical terms. These data is used as boundary conditions for the FSI tool. The model geometry is adapted according to the trim parameters, and then the performance of the new configuration is computed in real time.

Because of difficulties in dynamically measuring boundary conditions with precision and reproducing a manoeuvre in real time, only stationary conditions are analysed. This is an acceptable simplification because it can be assumed that, at the end of a manoeuvre, the sailing yacht operates in a quasi-stationary regime.

The resulting solver, named *Sailing*, provides real-time information (aerodynamic coefficients) about the trim and rigid structure to avoid problems such as breakage of the mast. Real-time monitoring is an innovation in navigation, especially in races.

Two of the most important requirements for *Sailing* are reduced computational cost and ability to adapt the analysis to the real position of sails. They are the main guidelines to select the calculation algorithms.

The two interconnected tools that make up *Sailing* are presented further in this paper.

The most relevant and original aspects of this work are the communication between the sensors and the FSI algorithm, and the methods to adapt the structure to real-time trim parameters. The sensors capture the trim parameters and these are communicated to the FSI algorithm to adjust the boundary conditions for structural analysis. That is, there is real-time consideration of the manoeuvre parameters in the determination of fluid-structure interaction. Near-time analysis is then conducted so that the results are immediately available to assist skippers in their decisions.

Next, simulation data are used to adjust an Artificial Neural Network in order to know in advance the best trim angle for certain wind conditions.

The FSI solver is coded in C++ and then the resulting code is integrated with the pre/post-process system GiD[1]. The FSI code is extended with a TCL[2] interface to provide the necessary communication routines with the sensor network.

The outline of this paper is as follows. In section 2, the FSI solver is presented. Section 3 focuses on the sensor network. The interface that connects the FSI program with the sensor network data is described in section 4. Section 5 gives some application examples. The paper ends with a discussion section and some conclusions.

2.   The fluid structure interaction solver

Sails are air foils that work by using an airflow set up by the wind and the motion of the boat. The performance of a specific sail configuration is obtained by the coupled effect of the airflow around the sails and structure response to the generated forces.

Rigging adjustments to achieve the desired amount of camber and twist are interrelated. That is the reason why structural analysis of all rigging elements in a fluid-structure interaction algorithm is necessary for the study of sail performance.

As said before, the FSI simulation algorithm integrates two solvers: (1) a fluid dynamics solver to calculate the aerodynamic forces for a given sail shape in upwind conditions; (2) a Finite Element Analysis (FEA) solver of the structural behaviour of rigging and sails. The aerodynamic forces and shroud and stay tension, as well as sheet tension, are taken into account.

---

[1] GiD: The universal, adaptive and user-friendly pre and postprocessor http://gid.cimne.upc.es/

[2] TCL: Tool Command Language http://www.tcl.tk/

In order to study sail and rigging performance of a boat, the first necessary step is the definition of the flying sail shape to be analysed. In this work, the flying sail is obtained by the fluid-structure interaction solver, but the iterative solution process starts with the designed sail plan geometry. A Graphic User Interface (GUI) based on GiD is developed to create or import the structure (sail and rigging) and define analysis data.

Flow and structural analysis, validation cases and interaction algorithm are detailed below.

2.1 Flow Analysis

The first numerical simulation of sails was conducted at the Massachusetts Institute of Technology in the 60s, when [14] developed Vortex Lattice Method (VLM) and flat wakes to investigate upwind sails. Since potential flow approximation is a reasonable approach for predicting upwind sail performance, provided that separation is restricted to small areas within the vicinity of the mast or leading edge, VLM is one of the computational methods commonly used to predict flow over sails [15, 16]. This method is relatively fast and suited for computing flow over combinations of highly cambered, thin lifting surfaces likes sails.

Provided that separation of the flow over the sail is restricted to small areas within the vicinity of the mast or leading edge, potential flow approximation is a reasonable approach. Thus, fluid flow must fulfil the Laplace equation as long as the boundary conditions are a zero normal velocity component and the Kutta condition at each trailing segment. The Laplace equation solution can be obtained by distributing elementary solutions over the problem boundaries (body surface S_B and wake surface S_w). In our case of study, the sail surface carrying the continuous distribution of doublicity is discretised into a set of vortex ring elements, each one carrying a locally constant value of doublicity (Γ). The Biot-Savart law is used to evaluate the velocity at each collocation point by each ring element. The boundary condition of zero normal velocity at each of the collocation points results in a set of algebraic equations. The solution of this set of equations results in the vector $(\Gamma_1, \Gamma_2, ..., \Gamma_m)$, which represents the doublicity of each ring element.

A preconditioned Bi-Conjugate Gradient method (BiCG) is used to solve the system of linear equations. Once the circulation of each singularity element is known, it is possible to calculate total flow velocity, pressures and loads.

[17] presented an alternative interpretation and implementation of the Vortex Lattice Method studied by [15]. The difference between this method and a general one, such as that proposed by [11], lies in the calculation of pressures and forces. The velocity induced by the doublicity distribution at the collocation point is split into two components: one normal $(u_{n,ind})$ to the surface (where n indicates the normal direction) and the other $(u_{m,ind}, u_{l,ind})$ in the tangent plane of the surface at the collocation point (where m and l indicate the two directions in the tangent plane of the surface). The free stream velocity, $\mathbf{Q}_\infty$, is transformed into the coordinates of the vortex ring element $\mathbf{Q}_\infty = (q_{m,\infty}, q_{l,\infty}, q_{n,\infty})$.

In order to obtain the velocity at the collocation point on both sides of the sail, half of the velocity jump is added to the mean velocity to give the upper surface velocity, and half of the velocity jump is subtracted to give the lower surface velocity. On the other hand, the velocity jump along direction s, which is $\partial\Delta\Gamma / \partial s$, is obtained using a simple finite difference approximation.

The free stream and the velocity induced by the doublicity distribution are combined with the velocity jump to obtain the velocity at each collocation point on both sides of the sail.

$$\mathbf{V}_{up} = \left(q_{m,\infty} + u_{m,ind} + \frac{1}{2}\frac{\partial \Delta \Gamma}{\partial m}, q_{l,\infty} + u_{l,ind} + \frac{1}{2}\frac{\partial \Delta \Gamma}{\partial l}, 0 \right) \tag{1}$$

$$\mathbf{V}_{down} = \left(q_{m,\infty} + u_{m,ind} - \frac{1}{2}\frac{\partial \Delta \Gamma}{\partial m}, q_{l,\infty} + u_{l,ind} - \frac{1}{2}\frac{\partial \Delta \Gamma}{\partial l}, 0 \right) \tag{2}$$

In this way, the method computes pressure at each side of the sail:

$$p_{up} = p_{\infty} - \frac{1}{2}\left(V_{up}^2 - Q_{\infty}^2 \right) \tag{3}$$

$$p_{down} = p_{\infty} - \frac{1}{2}\left(V_{down}^2 - Q_{\infty}^2 \right) \tag{4}$$

$$C_{up} = 1 - \left(\frac{V_{up}}{Q_{\infty}} \right)^2 \tag{5}$$

$$C_{down} = 1 - \left(\frac{V_{down}}{Q_{\infty}} \right)^2 \tag{6}$$

The method was codified into the solver to calculate coefficients and forces generated by a flow around a thin lifting surface.

Some validation cases were made to test the flow analysis. An example was the reproduction of an experiment carried out in the wind tunnel of the Chungnam National University of Korea [18]. The same geometry was tested using the flow analysis presented in this paper achieving an accuracy measurement of 90% for the lift and 75% for the drag.

2.2 Structural Analysis

The description of flow is supplemented by considering fluid-structure interaction. The particularity of sails is due to their high flexibility, and therefore a non-linear theory must be developed for the structural calculation [19, 20]. Rigging adjustments to achieve the desired amount of camber and twist are interrelated. That is why structural analysis of all rigging elements in a fluid-structure interaction algorithm is necessary for the study of sail performance.

Once the aerodynamic forces are evaluated, the next step is to compute the structure response to them. The method selected to analyse the structure and compute its response is the well-known Finite Element Method (FEM).

The rigging structure of a typical sailing yacht mainly consists of mainsail, jib, mast, spreaders, forestay, backstay, shrouds, main sheet and jib sheet. The different parts of the rigging and sails are modelled with membrane, truss and beam structural elements.

The solution algorithm is based on the minimisation of the potential energy. Potential energy E_{TOT} includes (a) the strain energy of elastic distortion $\phi(\mathbf{x})$, which is calculated depending on the type of element (membrane, cables and beams), and (b) the potential of applied loads Ω, by which they have the capacity to do work in case of displacement of the structure. The structures are analysed after each configuration change made by the crew, but the

resulting configuration is considered in a stationary state. Therefore, the equilibrium configuration is defined by the principle of stationary potential energy.

A description of all the elements is provided in the following subsections.

2.2.1 Sails

The behaviour of sails requires large displacement analysis of very thin structures. The models used to study sails are geometrically nonlinear, and since strains in modern sails remain low, constitutive laws of the material can be considered as linear, and stresses on the structure as linear functions of local strains. It is assumed that sails can be accurately modelled as membranes. Three-node triangular elements are used to discretise sails. The calculation method was presented by [21].

One of the validation tests was the reproduction of the Hencky's problem, which considers the deformation of an initially flat circular membrane with fixed edges, loaded with a constant pressure. The maximum deformation of the membrane reached 0.0330m in the centre part. This value almost matches the maximum deformation of 0.0331m obtained by Pauletti [22].

2.2.2 Cables

A sailboat's rigging is composed of many ropes and cables, mainly main sheet, jib sheet, forestay, backstay and shrouds. These elements can be modelled using bar finite elements. They can only transmit axial forces, which mean that the nodes of bar elements only have translational degrees of freedom. Therefore, it is possible to discretise a cable with a set of articulated bar elements. The resulting truss will be a cable that only transmits traction forces.

The model implemented in this work was presented by [23]. It includes a total Lagrangian description using the standard strain definition and assumes an elastic material. The cables are discretised with two-node linear elements, where the strain is assumed constant along the element and the material is considered to be homogeneous and isotropic.

The cables used in our structure are pre-stressed, as a result of the stress applied to trim the sail. This action leads to a cable strain. By exerting a constant stress on a cable element and considering a linear stress strain relationship, the potential strain energy and its gradient can be easily computed.

One of the validation cases considered a cable with fixed ends loaded with its own weight. Initially the cable had a V-shape, and the expected deformation was to obtain a U-shape. The reactions at the ends should be equal to the weight of the cable.

The properties of the material considered were $E=5.01 \cdot 10^6 N/m^2$ and $\rho=100 kg/m^2$, the length of the cable was L=14.1421 m and the area of the cable was A=0.0005 m^2. Considering the density of the material and the dimensions of the cable, the weight of the cable was P=69.36N. The reactions in each end were 34.681N and the total reaction was R=2·34.681=69.372N, obtaining the expected results.

2.2.3 Beams

The other elements of the structure (mast, spreaders and boom) resist axial and transversal forces, and bending moments. Therefore, they are modelled using beam theory [12, 24]. The beams are modelled as a two-node beam element with six degrees of freedom per node. The mast and the boom are connected by a hinge to allow rotation of the boom around the mast. To introduce the capability of releasing a degree of freedom, the algorithm presented in [25] to obtain the condensed stiffness matrix is adapted to simulate the hinge between the mast and the boom.

One of the validation cases was the simulation of a vertical cantilever with a horizontal load. The problem had the following parameters: length L=14m, A=21.36cm^2, I$_x$=5.8·10^{-6}m^4, I$_y$=1.35·10^{-5}m^4, J=1.9·10^{-5}m^4, G= 3.946·10^{10} N/m^2 and E=1.105·10^{11}N/m^2.

The lowest node had restricted translations and rotations in all directions, and the top node had a punctual load of 500 N applied in the x direction.

It was possible to calculate the displacement of the top node with the following analytical expression:

$$Y_{max_0} = \frac{F \cdot L^3}{3 \cdot E \cdot I_y} = \frac{500 \cdot 14^3}{3 \cdot 1.105 \cdot 10^{11} \cdot 1.35 \cdot 10^{-5}} = 30.7 cm \tag{7}$$

The displacement of the top node obtained was 30.6 cm and the reaction was R=500N, which are both expected results.

2.2.4 Equilibrium configuration

The solution procedure involves generating the structure model with the above elements, imposing boundary or support conditions and solving the equations to obtain nodal quantities by imposing the minimisation of the potential energy.

A conservative mechanical system has an energy potential, E_{TOT}, which includes the strain energy of elastic distortion $\phi(\mathbf{x})$ and the potential of applied loads Ω.

In the problem at hand, the airflow applies external loads on the structure, causing the displacement and strain of the elements. Given the nodal displacement vector $\mathbf{x}$ and nodal flow forces $\mathbf{f}$, the potential of applied loads is $\Omega = -\mathbf{f}^T \mathbf{x}$.

The strain energy $\phi(\mathbf{x})$ is calculated according to the finite element analysed (membrane, truss or beam).

The total potential energy is

$$E_{TOT} = \sum_{elements} \phi(\mathbf{x}) - \mathbf{f}^T \mathbf{x} \tag{8}$$

And thus the equilibrium configuration is found from the stationary value of the total potential energy:

$$\frac{\partial E_{TOT}}{\partial \mathbf{x}} = \sum_{elements} \nabla \phi(\mathbf{x}) - \mathbf{f} = 0 \tag{9}$$

This non-linear system of equations is solved by a Quasi-Newton iterative procedure. The computer code uses the limited memory Broyden-Fletcher-Goldfarb-Shanno method (BFGS) to tackle large scale problems, as described by [26]. A line search procedure as described by [27] is implemented, too.

2.3 Fluid-Structure Interaction Algorithm

Complete modelling of sail steady equilibrium involves a fluid-structure interaction analysis. The presence of the sail modifies the flow, whilst the latter applies aerodynamic forces on the former, changing its geometry.

[28, 29, 30, 31] dealt with the numerical problem by coupling FEM and VLM solvers. [32] pointed out that one of the reasons for poor convergence of the FEM-VLM is the use of the same discretisation scheme for the FEM and VLM. That is why this work uses different discretisation schemes for these solvers.

The VLM selected to compute flow forces on the sails uses quadrilateral elements, even though these elements can create both structured and unstructured meshes. The membrane element selected to compute sail response is based on three-node triangular elements. In order to fulfil the requirements of both methods, a structured mesh of quadrilateral[3] elements is generated and split internally by the program into triangular elements (Fig. 1). This procedure allows the two meshes to have coincident nodes facilitating data transfer between the two meshes.

Elements for the VLM   Elements for the FEM
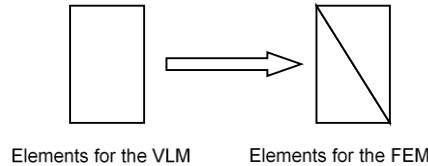
Fig. 1 Fluid Solver mesh and Structural Solver mesh

This fluid-structure interaction method is iterative: starting from an initial geometry, the flow forces are calculated, from which sail displacements are then evaluated, and finally the flow simulation is repeated with the updated geometry and the structural calculation is in turn repeated with the updated flow forces until convergence is achieved. The grid is thus modified at each fluid-structure iteration. Lagrangian advance techniques are used to fit the sail grid surface from the deformed sail calculated in the previous iteration. Lagrangian updating of the grid is done automatically by the algorithm as a hidden procedure for users.

The first step of the calculation is to apply the trim parameters to the basic structure as initial loads and boundary conditions. In order to modify these parameters in execution time, a TCL interface is implemented. This interface includes several communication routines allowing solvers to be connected with a network of sensors located on the rigging to obtain the trim parameters in real time.

From the interaction method in [33], an embedded iteration scheme is used to achieve convergence of the iterative procedure of the potential flow solution process, as well as the solution of the non-linear system of equations to calculate equilibrium in the structural code. External flow is computed by taking into account the sail configuration (aerodynamic step). Once the flow field is given, the new configuration is computed (structural step). This leads to a new external flow because of the updated geometry of the sail and so on. The sequence of aerodynamic/structural steps is repeated until the stopping condition is satisfied.

If the difference between the nodal forces computed at two consecutive iterations of the flow solver is less than a tolerance, it is sufficient to consider that the change in geometry will be small compared to the previous step. Then, the stopping criteria will be met. Since k and $k+1$ are two consecutive iterations between the fluid solver and the structural solver, the stopping criteria will be

$$\forall node \frac{\left|\mathbf{f}_{k+1}-\mathbf{f}_k\right|}{\left|\mathbf{f}_k\right|} < tol \qquad (10)$$

Different numerical tests showed that a tolerance of 0.1 has little influence on the result. In practice, most nodes have small change ($1\cdot10^{-5}$-$1\cdot10^{-8}$). The error norm is usually defined by the nodes at the upper end of the mainsail, where the results of two consecutive iterations differ more than for the other sail nodes.

The scheme of the calculation process, including the grid updating algorithm inserted in the iteration process between the fluid solver and the structural solver, is shown in Fig. 2.
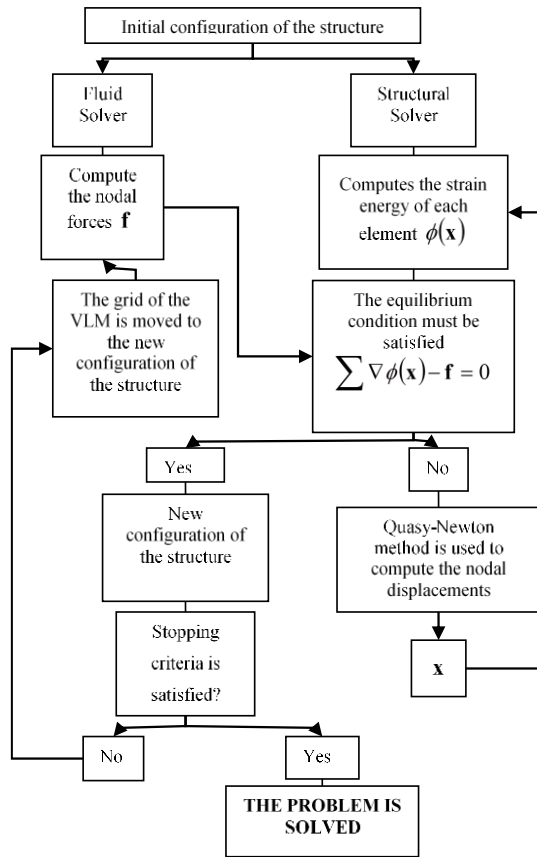
```
                    Initial configuration of the structure

          Fluid                              Structural
          Solver                               Solver

         Compute                        Computes the strain
        the nodal                        energy of each
        forces f                         element φ(x)

      The grid of the                   The equilibrium
       VLM is moved to                   condition must be
       the new                            satisfied
       configuration of                  ∑ ∇φ(x) − f = 0
       the structure

              Yes                              No

             New                          Quasy-Newton
        configuration of                  method is used to
          the structure                   compute the nodal
                                          displacements

          Stopping                              x
          criteria is
          satisfied?

        No            Yes

                THE PROBLEM IS
                   SOLVED
```

Fig. 2 Fluid-Structure interaction algorithm

3. Monitoring System

Despite the efforts invested in the development of monitoring systems for racing yachts in the last decades, to the author's knowledge, no flexible system able to be adapted to any rigging design and measure the structural response of elements and identify current operating configurations in real time is yet available. Therefore, a new monitoring system was developed [34].


Fig. 3 Sensor element for monitoring traveller position (3DRRM)

The electronics of the device are based on the platform Waspmote[3], commercialised by Libelium. The sensor, named '3D Remote Rigging Monitor' or 3DRRM (Fig. 3), was designed to measure stress on any rigging element.

Experimental tests were designed to demonstrate that standard instrumentation using strain gauges is sensitive enough to accurately monitor current rigging elements. Furthermore, it was necessary to proof whether the output obtained by these means was also sensitive to the orientation between the gauge and the principal strain directions.

Eight strain gauges configured in two full Wheatstone bridges were installed in the 3DRRM. Different tensile tests were carried out to evaluate the operation of the device, showing a positive performance in all tested cases. Experimental setup for these two configurations is shown in Figure 4.
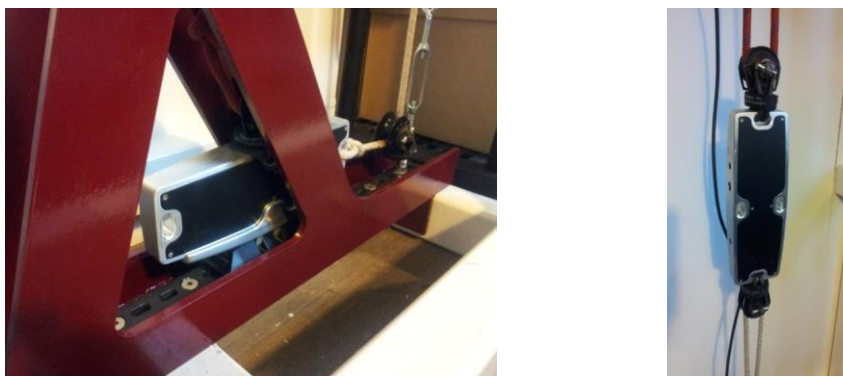
Fig.4 Experimental setup of 3DRRM tests (configuration modes: Force and Angle, left image, and Force, right image)

The designed sensors could process measured strain data by applying Artificial Neural Networks (ANN) algorithms [35, 36] to unambiguously establish the direction and magnitude of the traction force acting on the element. The function to be approximated by the ANN in this case had two inputs (strains ε_1 ε_2, measured on each side of the device) and two outputs; load and pull angle of the sheet $\{\mathbf{F}, \alpha\} = f(\varepsilon_1, \varepsilon_2)$.

The ANN structure used had one hidden layer of perceptron neurons. The learning/validation was carried out for different number of neurons in the hidden layer. The best fitting with the validation data was the criteria used to select the optimum number.

To test the neural network, 320 FEM analysis and 76 points obtained in the laboratory tests were made available. For the validation task, 80% of the simulation data and 46 points of the experimental data were selected randomly as training data. The remainder data was used for validation purposes. The training data was used to adjust the hidden internal parameters of the neural network. Once the neural network was adjusted to the data, it was executed with the inputs of the validation data, and these results were compared with the validation data results. This comparison was done by creating a linear regression and calculating the coefficient of determination.

---

[3] Waspmote http://www.libelium.com/products/waspmote

Several network configurations were used but the optimal fitting was obtained with four neurons at the hidden layer. The neural network fitting was almost perfect, obtaining a coefficient of determination of 0.996.

This way, it was possible to identify the operating conditions of the rigging.

4. Integration of a monitoring system with the FSI Algorithm

As stated above, our main goal was to develop a near-time simulation tool of the behaviour of sails and rigging to help the crew optimise real-time yacht performance. To do this, the actual configuration of the sail structure must be known in advance.

The parameters defining this configuration are the so-called trim parameters. The trim parameters considered in this work are angle to the wind, backstay load, forestay load, shroud load, main sheet load and angle, and jib sheet load and angle.

Shroud and stay stress is adjusted at dock. During sailing, the crew trim the sails by varying traveller position (twist) and adjusting sheet stress (camber). Structural and potential flow calculation depends on these adjustments. Their initial values are inserted into the GUI as initial data. This information is used to update the geometry and then compute the performance of this new configuration with the coupled fluid-structure interaction algorithm.

To measure the trim parameters, a 3DRRM [34] element is attached to any rope or cable of the sailing yacht (main sheet, jib sheet, shrouds or stays) for monitoring. The wireless monitoring elements provide the trim parameters (shroud load, stay load, main sheet load and angle, jib sheet load and angle, main traveller and jib traveller position) applied by the crew and the wind intensity and angle.

Data acquired by the WSN are transmitted to perform the aerodynamics/structural calculation via a C++ interface to interpret TCL scripts. This information is used as inputs and boundary conditions to the calculation/simulation system. The TCL interface reads the 'external initial conditions' and calls the C++ functions required to update the geometry. Furthermore, this system can access 'real time' data obtained by the WSN and update the boundary conditions to be used by the FSI solver accordingly.

Shroud load, stay load, main sheet load and jib sheet load exert a constant stress on cable elements. In addition, when the crew move the travellers (main traveller and jib traveller), their angle must be 'virtually' reproduced by our geometry. In order to introduce in our solver provide our solver with the capability to adapt sail position into the solver, an algorithm was created using the ideas in [34]. A particular sail trim is carried out by wrapping the jib sheet around the forestay and the mainsail around the mast.

Trim performance is analysed for a certain wind condition and structure configuration. If the wind condition changes or the crew change the structure configuration, a new performance analysis will be made. A rigging monitoring tool able to communicate in real time with the FSI solver is designed. This tool allows finding the boundary conditions which define the new structure configuration. Using these data, the performance of this trim is computed. Some validation cases were carried out to verify the results of this tool.

5. Results. An application case

One of the original aspects of the program is the communication between the sensors and the FSI algorithm. The sensors capture the trim parameters, which are communicated to the FSI algorithm for their adjustment. However, the performance of the complete tool cannot be validated with experimental data because these are very scarce. This is mainly due to two factors: (a) the difficulty in measuring the deformed shape of sails and the wind pattern producing the strain, and (b) the transient character of the phenomena involved, which makes

the measurement of the exact instantaneous sail shape/wind pattern difficult. Performing a full scale test of sails and rigging is out of the question due to the dimensions necessary for the wind tunnel. Also, a model test would not be reliable for full scale extrapolation due to the difficulty in simulating sail and rigging elasticity. Thus, the benchmark validation performed in this work is the only way to check results. In the case under study, the accuracy of this model could be sufficient for practical purposes.

The application examples presented in this section are based on the Totalboats GP42 yacht, where the WSN was tested. The sail plan geometry and rigging of this boat were reproduced in our pre-processor system GiD (see Fig. 6). Next, the required structural properties of every element, the boundary conditions (desk nodes, free rotating nodes such as the join between the mast and cable element loads) and other data were entered.
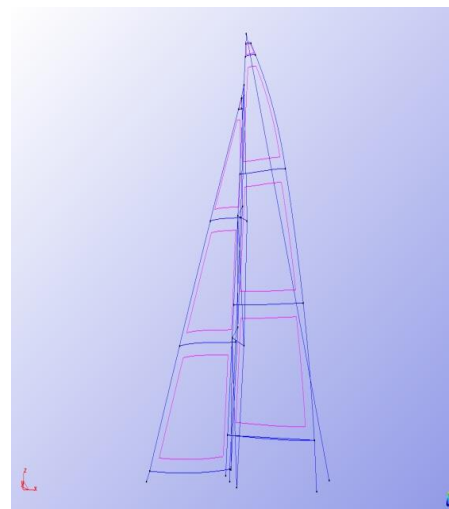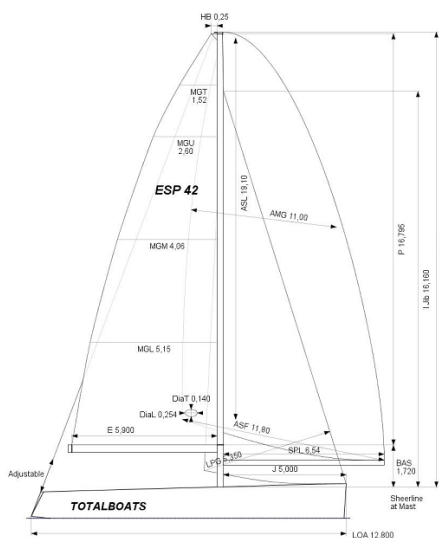
Fig. 5 Model of the GP42. Source Totalmar   **Fig. 6** Model of the GP42 in GiD

Case 1

The following parameters were used for rigging case:

- Apparent wind velocity is 8 m/s and apparent angle is 15°.

- Main traveller position is (6.22, 0.34, -0.59). Hence, mainsail trim angle is $\delta_F = 3.25°$.

- Jib traveller position is (0.41, 0.88, -0.50). Hence, jib trim angle is $\delta_M = 8.9°$.

- Main sheet and jib sheet loads are 1500 N and 700 N, respectively.

- Backstay load is 10000 N.

- Forestay load is 20000 N.

- Shroud load is 1000 N.

The results for this first configuration with an apparent wind angle of 15° are shown in Fig. 7.
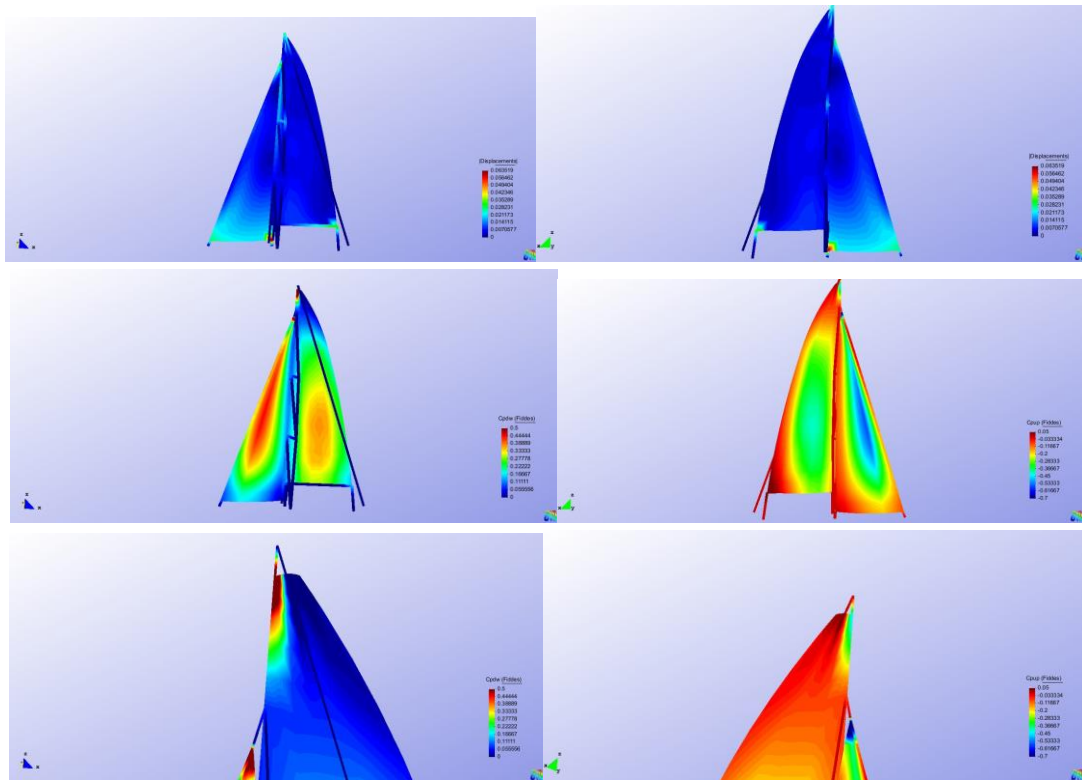
Fig. 7. Results for the first configuration: Displacements, Cp and abnormal area for an apparent wind angle of 15º
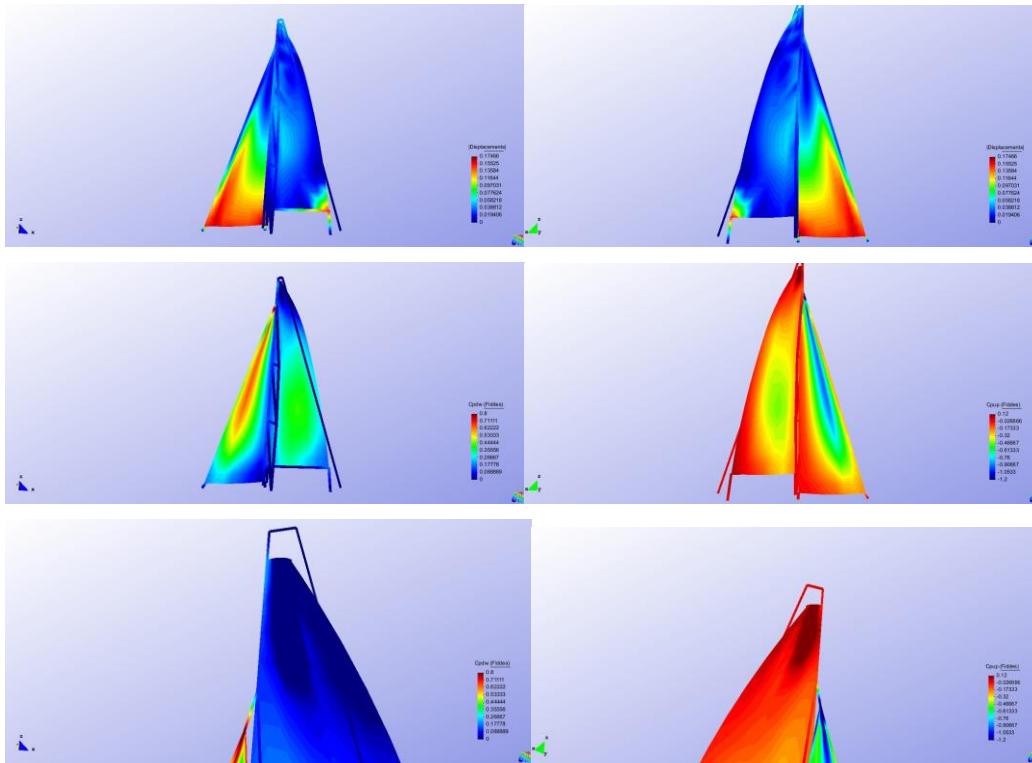
Areas where the pressure coefficient has an abnormal value, i.e. a negative value, are worth noting. This abnormal value can be attributed to two reasons: flow is turbulent or separated in these areas or these areas are flapping.

In order to study the effect of apparent wind angle, in the second configuration, the apparent wind angle is 20°. The wind condition then changes, and therefore the crew trim the sails. The new trim parameters are detected by the integrated WSN:

-   Apparent wind velocity is 9 m/s and apparent angle is 20°.

-   Main traveller position is (6.22, 0.63, -0.59).

-   Jib traveller position is (0.37, 1.095, -0.5).

-   Main sheet and jib sheet loads are 2000N and 1000N, respectively.

-   Shroud load is 1200 N.

-   Backstay load is 15000 N.

-   Forestay load is 22000 N.

These changes are introduced into *Sailing* by the TCL interface and the 'virtual geometry' is adjusted to these trim parameters. The performance of this new configuration is then computed.

The response of this structure is shown in Fig. 8.

Fig. 8 Results for the second configuration: Displacements, Cp and abnormal area for an apparent angle of 20º

It is possible to see the changes in the pressure coefficient and the areas with abnormal values.

Case 1 proves the versatility of the 3DRRM. The different configurations (shrouds, backstay, forestay, main sheet and jib sheet) were presented and analysed to obtain loads at each one of them by the 3DRRM. In this way, all the rigging elements could be monitored.

Data obtained by the 3DRRM were communicated through the TCL interface, and the geometry could be virtually trimmed. FSI software calculation was executed with the new parameters to determine the appropriateness of the model.

Case 2

Separated or turbulent flow around the head of the sails is related to the effect of jib trim angle δ_J and mainsail trim angle δ_M. Marchaj [37] suggested that the best position for the foresail relative to the mainsail and its trim angle varies with the apparent wind angle. The recommended close-hauled angle of the foresail trim was $7º < \delta_J < 20º$. After several tests at Southampton University wind tunnel, Marchaj proved that, in order to obtain high aerodynamic efficiency, flow on the leeward side of the sail must be attached and steady. These tests demonstrated that at the small apparent wind angle of 20°, when $\delta_J = 10º$ and $\delta_M = 5º$, attached flow is around most of both sails, and when the apparent wind angle increases to 25° and the trim angles are the same, turbulent or separated flow regions increase.

Considering this and maintaining the values of the rest of variables and varying the apparent wind angle, the influence of jib trim angle, δ_F, is evaluated:

- Apparent wind velocity is 8 m/s.

- New main traveller position is (6.22, 0.63, -0.59). Mainsail trim angle is $\delta_M = 5.78°$.

- Main sheet and jib sheet loads are 2000N and 1500N, respectively.

- Shroud load is 1200 N.

- Backstay load is 15000 N.

- Forestay load is 22000 N.

The driving force for different apparent wind angles is shown in Fig. 9.
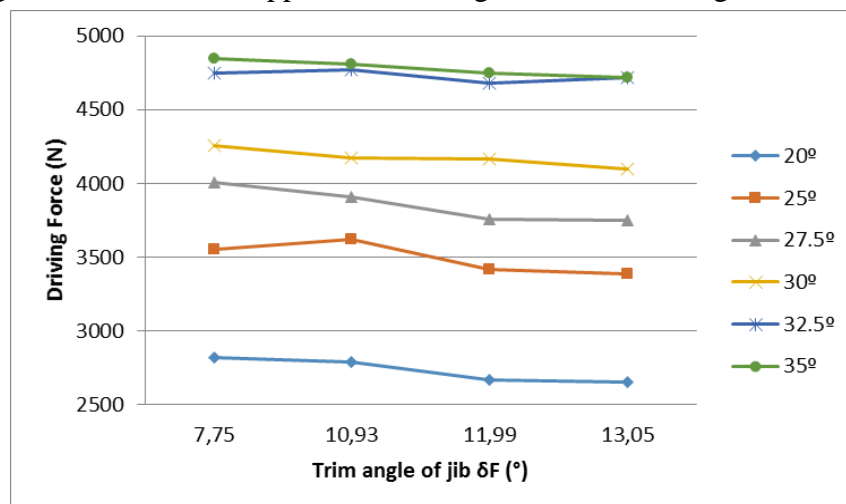
Fig. 9 Driving Force when varying jib trim angle for different apparent wind angles

As can be seen in Fig. 9, higher driving forces are obtained for jib trim angles closer to the centre line of the ship and larger apparent wind angles. It is important to emphasise that the program is intended for use in upwind conditions; therefore, the angles of incidence must be less than 35°. Apparent wind angles of 50° and 60° are too large to be considered as close hauled sailing. For these angles, flow is usually not attached to the sail and the approximation of potential flow is not correct.

Moreover, when δ_J is larger than 10°, the driving force decreases, which could be explained by Marchaj's theory.

Example 2 shows calculations to generate a driving force database based on trim parameters and wind conditions for the development of a Decision Support System (DSS) to help skippers during navigation.

6. Conclusions

The main objective of our work was to develop a simulation program of the behaviour of sails and rigging to help the crew optimise real-time yacht performance and prevent accidents. For this purpose, a tool named *Sailing* integrating a fluid solver, a structural solver and a TCL communication interface with a wireless rigging monitoring system was designed. This tool is able to compute the performance of sail/rigging configurations and monitor the state of the rigid structure.

A flexible sensor, 3DRRM, was developed to measure stress on any rigging element of the boat. The concept of the sensor is based on measuring strain at different points of the device. These strain values are processed to unambiguously establish the direction and magnitude of the traction force acting on the element.

A network of these sensors can be integrated with the FSI solver by means of a TCL communication interface. Using the information from the WSN, the trim parameters are entered into the solver as boundary conditions.

Sailing provides the crew with real-time information (aerodynamic coefficients) to help them find the best trimming conditions, just like a DSS. Additionally, it informs about the state of the rigid structure to prevent accidents. Real-time monitoring is an innovation for navigation, especially for races.

Sailing can also perform different simulations by systematically varying trim parameters to obtain a database of structure and driving force responses depending on wind conditions and trim parameters. This database would be the first step to develop a decision support system. With this DSS, sailing yacht skippers would be able to decide in advance the optimum trimming for a specific wind condition.

7. ACKNOWLEDGEMENTS

REFERENCES

[1] Zamarin, A., Matulja, T. and Hadjina, M. (2013) Methodology for Optimal Mast and Standing Rigging Selection of a Racing Yacht Using AHP and FEM. Brodogradnja, 64(1), 11-21.

[2] Park, J.-H., Storch, R.L. (2002). Overview of ship-design expert systems. Expert Systems with Applications, 19(3), 136-141.

[3] Arendt, R. (2004). The application of an expert system for simulation investigations in the aided design of ship power system automation. Expert Systems with Applications, 27(3), 493-499.

[4] Arendt, R., van Uden, E. (2011). A decision-making module for aiding ship system automation design: A knowledge-based approach. Expert Systems with Applications, 38(1), 410-416.

[5] Kowalski, Z., Arendt, R., Meler-Kapcia, M., Zielnski, S. (2001). An expert system for aided design of ship systems automation. Expert systems with Applications, 20(3), 261-266.

[6] Kowalski, Z., Meler-Kapcia, M., Zielinski, S., Drewka, M. (2005). CBR methodology application in an expert system for aided design ship's engine room automation. Expert systems with Applications, 29(2), 256-263.

[7] Fagerholt, K. (2004). A computer-based decision support system for vessel fleet scheduling- experience and future research. Decision Support Systems, 37(1), 35-47.

[8] Calabrese F., Corallo A., Marghenta A., Zizzari, A.A. (2012). A knowledge-based decision support system for shipboard damage control. Expert systems with Applications, 39 (9), 8204-8211.

[9] Keebber, B., Hochkirch, K. (2006) Numerical investigation on the effects of trim for a yacht rig. Proceedings on 2nd High Performance Yacht design Conference. Auckland, Australia.

[10] Runnerstrom, E. (2003). Human systems integration and shipboard damage control. Naval Engineers Journal, 115(4): 71-80.

[11] Katz, J., Plotkin, A. (2006). Low speed aerodynamic (2nd edition) New York: Cambridge University Press. ISBN-13 978-0-521-66219-2.

[12] Oñate, E. (2009) Introduction to the finite element methods for structural analysis. Linear static. Springer and CIMNE, Barcelona.

[13] Zienkiewicz, O. (1982) El método de los elementos finitos. Reverte, Barcelona.

[14] Milgram, J. (1968). The aerodynamics of sails. Proceedings of the 7th Symposium of Naval Hydrodynamic. 1397-1434.

[15] Jackson, P.S., Fiddes, S. (1995). A new view of the vortex lattice method. Technical Report. University of Bristol, Department of Aerospace Engineering.

[16] Couser, P. (1998) Computational methods for investigating sail forces – a case study. Proceedings of Yacht Vision.

[17] Fiddes, S., Gaydon, J. (1996) A new vortex lattice method for calculating the flow past yacht sails. Journal of Wind Engineering and Industrial Aerodynamics, 63(1-3), 35-60.

[18] Yoo J. and Kim, H.T. (2006) Computational and experimental study on performance of sail of a sailing yacht. Ocean Engineering, 33, 1322-1342.

[19] Jackson, P.S. (1983). A simple model for elastic two-dimensional sails. AIAA Journal, 21(1), 153-155.

[20] Jackson, P.S. (1985). The analysis of three-dimensional sails. Proceedings of the 10th Canadian Congress of Applied Mechanics. Ontario, Canada.

[21] Arcaro, V. (2004a) A simple procedure for shape finding and analysis of fabric structures. UNICAMP/FEC Web. http://www.arcaro.org/tension/main.htm. Accessed 2010.

[22] Pauletti R.M, Mariani Guninardi, D. and Camilo Deifeld, T.E. (2005) Argyris Natural Membrane Finite Element. Barcelona : STRUCTURAL MEMBRANES CIMNE, 2005.

[23] Arcaro,V. (2004b) A simple procedure for analysis of cable network structures. UNICAMP/FEC Web. http://www.arcaro.org/tension/main.htm. Accessed 2010.

[24] Cook, R., Malkus, D., Plesha, M., Witt, R. (2002) Concepts and applications of finite element analysis. John Wiley and Sons, Wisconsin.

[25] Cook, R. (1995) Finite Element Modeling for Stress Analysis. John Wiley and Sons, New York.

[26] Nocedal, J., Wright, S. (1999) Numerical optimization. Springer-Verlag.

[27] Gill, P., Murray, W. (1974) Newton type methods for unconstrined and linearly contrained optimization. Mathematical Programming, 7, 311-350.

[28] Jackson, P.S., Christie, G. (1987) Numerical analysis of three-dimensional elastic membrane wings. AIAA Journal, 25(5), 676-682.

[29] Schoop, H. (1990) Structural and aerodynamic theory for sails. European Journal of Mechanics, A/Solids, 9(1), 37-52.

[30] Muttin, F. (1991) Structural analysis of sails. European Journal of Mechanics, A/Solids, 10(5), 517-534.

[31] Fukasawa, T., Katori, M. (1993) Numerical approach to aeroelastic response of three-dimensional flexible sails. Proceedings of the 11th Chesapeakes Sailing Yacht Symposium.

[32] Schoop, H., Bessert, N. (2001) Instationary aeroelastic computation of yacht sails. International Journal for numerical methods in engineering, 52, 728-803

[33] Renzsch, H., Müller, O., Graft, K. (2008) FlexSail: A fluid-structure interaction program for the investigation of spinnakers. Proceedings in the International Conference on Innovations in High Performance Sailing Yachts.

[34] García, J., Ortigosa, I. and Fernández, A. (2015) Development of a Decision Support System for Optimization of the Performance of Sailing Yachts. Revista Internacional de Métodos Numéricos para Cálculo y Diseño en Ingeniería, 31 (3), 146-153.

[35] Haykin, S. (1999) Neural Networks – A Comprehensive Foundation (2nd ed), USA: Prentice-Hall Inc.

[36] Graf, K., Renzsch, H. (2006) RANSE Investigation of Downwind Sails and Interaction into Sailing Yacht Design Process. Proceedings in 2nd High Performance Yacht Design Conference.

[37] Marchaj C.A. (2003) Sail Performance. techniques to Maximise Sail Power. Adlard Coles Nautical. ISBN 0-7136-6407-X.